Missense mutations in the dopamine transporter gene associate with adult parkinsonism and ADHD

Supplementary Information

Freja H. Hansen[1*], Tina Skjørringe[2*], Saiqa Yasmeen[2], Natascha V. Arends[1], Michelle A. Sahai[3], Kevin Erreger[4], Thorvald F. Andreassen[1], Marion Holy[5], Peter J. Hamilton[4], Viruna Neergheen[6], Merete Karlsborg[7], Amy H. Newman[8], Simon Pope[6], Simon JR. Heales[6, 9], Lars Friberg[7], Ian Law[10], Lars H. Pinborg[11], Harald H. Sitte[5], Claus Loland[1], Lei Shi[3], Harel Weinstein[3], Aurelio Galli[4], Lena E. Hjermind[12†], Lisbeth B. Møller[2†]
& Ulrik Gether[1†]

[1]Molecular Neuropharmacology Laboratory, Department of Neuroscience and Pharmacology, Faculty of Health and Medical Sciences, University of Copenhagen, Copenhagen, Denmark, [2]Center for Applied Human Genetics, Kennedy Center, Copenhagen University Hospital, Glostrup, Denmark, [3]Department of Physiology and Biophysics, Weill Medical College of Cornell University, New York, USA, [4]Department of Molecular Physiology & Biophysics, Vanderbilt University, Nashville, USA, [5]Medical University of Vienna, Center for Physiology and Pharmacology, Institute of Pharmacology, Vienna, Austria, [6]Neurometabolic Unit, National Hospital for Neurology & Neurosurgery, London, UK, [7]Department of Neurology, Bispebjerg Hospital, Copenhagen University Hospital, Denmark, [8]National Institute on Drug Abuse-Intramural Research Program, National Institutes of Health, Baltimore, USA, [9]Chemical Pathology, Great Ormond Street Hospital for Children, London, UK, [10]Department of Clinical Physiology, Nuclear Medicine and PET, Rigshospitalet, Copenhagen University Hospital, Copenhagen, Denmark, [11]Neurobiology research unit, Epilepsy Clinic, Copenhagen University Hospital, Denmark, [12]Danish Dementia Research Centre, Clinic of Neurogenetics, Department of Neurology, Rigshospitalet, Copenhagen University Hospital and Department of Cellular and Molecular Medicine, Section of Neurogenetics, Faculty of Health and Medical Sciences, University of Copenhagen, Copenhagen, Denmark.
* These authors contributed equally to this work
† These authors contributed equally to this work

Correspondence:

Ulrik Gether, MD, Professor
Molecular Neuropharmacology Laboratory
Department of Neuroscience and Pharmacology
The Faculty of Health and Medical Sciences
University of Copenhagen, DK-2200 Copenhagen N, Denmark
Tel: +45 2384 0089; Fax: +45 3532 7610; E-mail: gether@sund.ku.dk

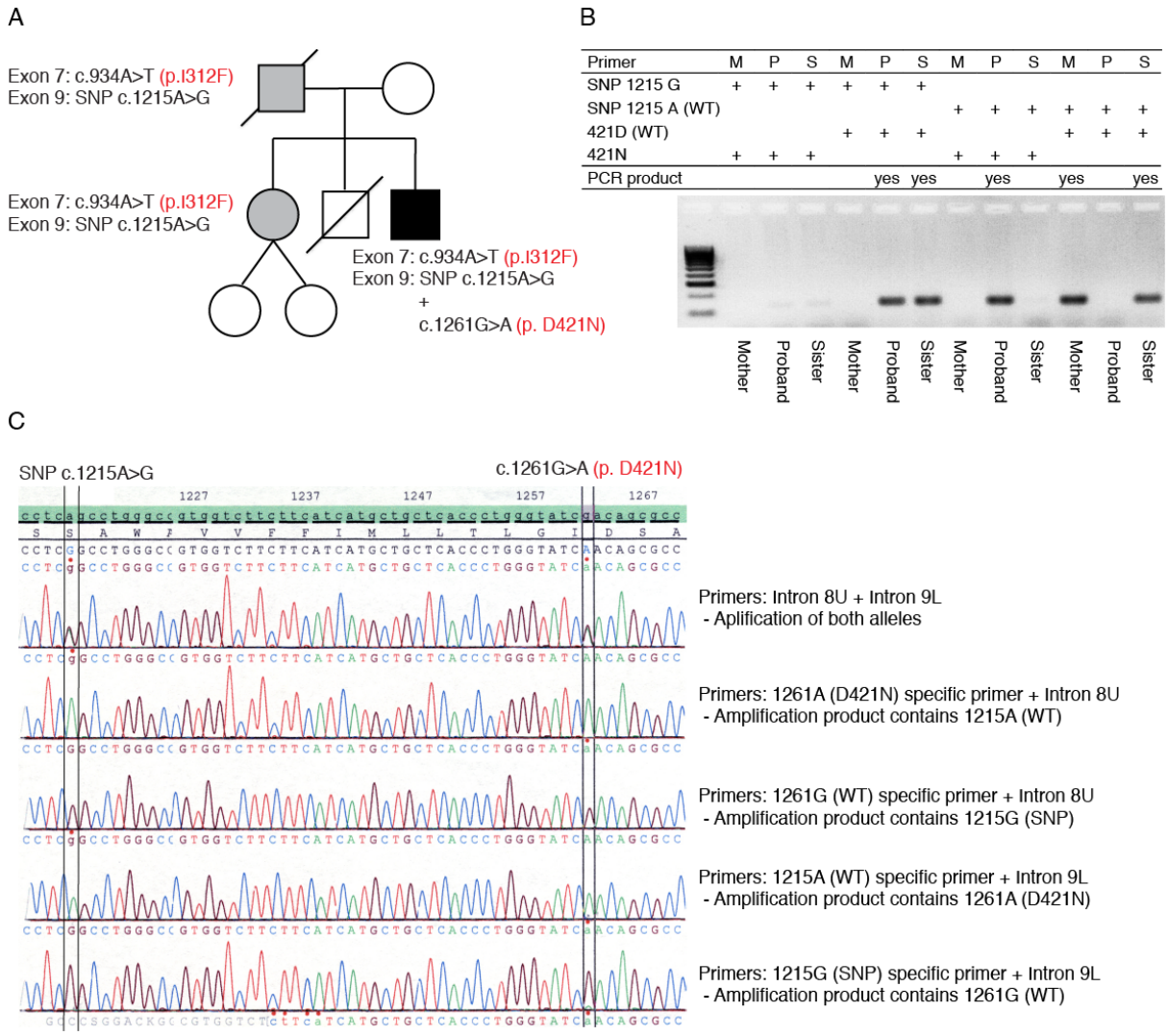

Supplementary Figure S1

A) Pedigree analysis demonstrating the carrier status of the D421N (c.1261G>A) and I312F (c.934A>T) mutations along with a SNP, c.1215A>G (p. S405S), in exon 9. The proband and his sister carry the DAT-I312F in exon 7 variant and the c.1215A>G SNP in exon 9. The proband also carries the DAT-D421N mutant in exon 9. As the mother only carries WT alleles, the allele containing both the I312F mutation in exon7 and the c.1215A>G SNP in exon 9 has presumably been transmitted to both siblings from the diseased father. Hence, D421N appears to be the result of a *de novo* mutation. **B)** Analysis of *cis/trans*-position of the D421N mutation and the I312F mutation. To investigate if the I312F and D421N mutations are positioned on separate alleles in the proband, we took advantage of the c.1215A>G SNP in exon 9, which co-segregates with the I312F mutation. We performed PCR experiments on genomic DNA from the proband (P), his mother (M), and his sister (S) in the presence of sequence specific primers designed to recognize either the D421N mutation or the

c.1215A>G SNP, by variation of the most 3´terminal base. The sequence of the primers annealing to c.1215A/G is: 5'-ACGCTCCCTCTGTCCTC**A/G**-3' and the sequence of the primers annealing to c.1261G/A (D421N) is 5'-GTTACTCACGGCGTGT**C/T**-3' (complementary strand). The table summarizes the PCR results obtained with the 4 combinations of WT sequence and mutant/SNP sensitive primers and the gel image below visualizes the resulting amplification of DNA. The data demonstrate a DNA amplification pattern that is consistent with *trans*-position of the D421N mutation and the c.1215A>G SNP. Thus, amplification of genomic DNA from the proband does not occur when performing the PCR with both the D421N and the c.1215A>G selective primers. Accordingly, the data provides evidence for a trans-position of the I312F and D421N mutations in the patient. The PCR were performed using Hot Start 95^{o}C 15 min followed by 35 cycles (95^{o}C (1 min), 67 ^{o}C (1 min), 72 ^{o}C (7 min)) and 7 min 72 ^{o}C. In addition to the sequence specific part of the primers all forward primers were extended (5' end) with the sequence acccactgcttactggcttatc and all reverse primers with the sequence gaggggcaaacaacagatggc in order to extend the products. **C)** Amplification of the two different DNA strands, using primers specific for either the 1215A>G SNP or the 1261G>A (D421N) mutation, in combination with primers in intron 9L or 8U respectively. Upon sequencing of the amplified PCR products we again observed that the D421N mutation and the 1215A>G SNP were positioned on separate alleles, which provides further support for the *trans*-position of D421N and I312F mutations. The applied primers have the following sequences:

Intron 8U: acccactgcttactggcttatcagaaaggggctttcagc

Intron 9L: gaggggcaaacaacagatggcaggggataaagggaaaggt

1261G (WT): gaggggcaaacaacagatggcgttactcacggcgctgtC

1261A (D421N): gaggggcaaacaacagatggcgttactcacggcgctgtT

1215A (WT): acccactgcttactggcttatcACGCTCCCTCTGTCCTCA

1215G (SNP) acccactgcttactggcttatcACGCTCCCTCTGTCCTCg

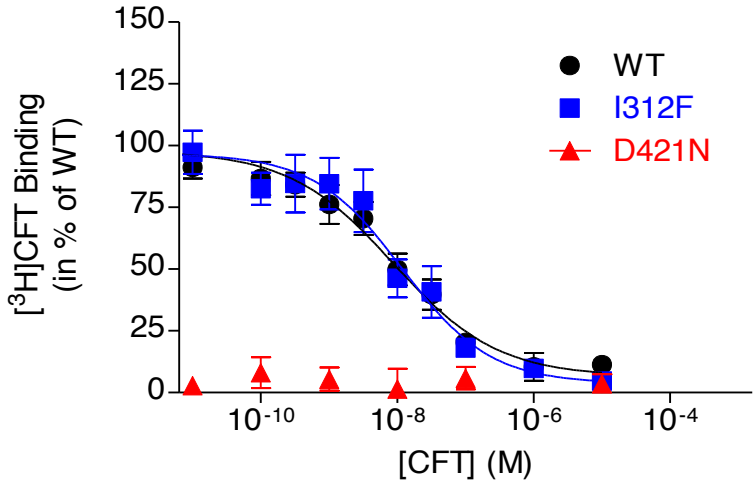

Supplementary Figure S2

[^{3}H]-CFT binding to transiently transfected HEK293 cells. The curves are averages of 3-5 experiments, each performed in triplicates or hexaplicates. Binding data was fitted by nonlinear regression and normalized to WT in each experiment. Whilst DAT-I312F shows preserved binding properties (IC50 ± s.e.m. of the presented curves are 13.3±1.5 nM and 11.8±1.9 nM for WT and DAT-I312F respectively), no specific binding to DAT-D421N was detected. Of notice, we observed a markedly higher non-specific binding in HEK293 cells compared to COS-7 cells and consequently an impaired assay window.

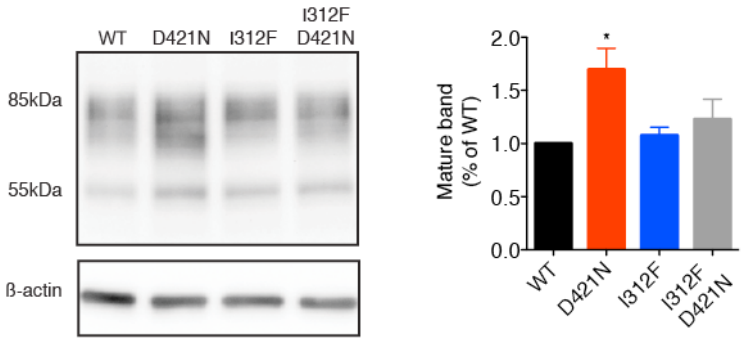

Supplementary Figure S3

Expression of DAT mutants in HEK293 cells. The left panel shows a representative immunoblot of DAT content in HEK293 cells, transiently transfected with WT, DAT-D421N, DAT-I312F, or both DAT-D421N and DAT-I312F, keeping the amount of DNA used for transfection constant. Both WT and mutants elute as two bands, representing the mature and the immature glycoforms of ~80kDa and ~55kDa respectively. ß-actin has been used as loading control. The right panel shows quantification of the mature DAT glycoforms as percentage of WT. DAT-D421N has significantly increased levels of the mature glycoforms compared with WT, whereas levels of mature DAT-I312F are comparable to WT. Data are means ± s.e.m, n=5, one-sample t-test, *p<0.05.

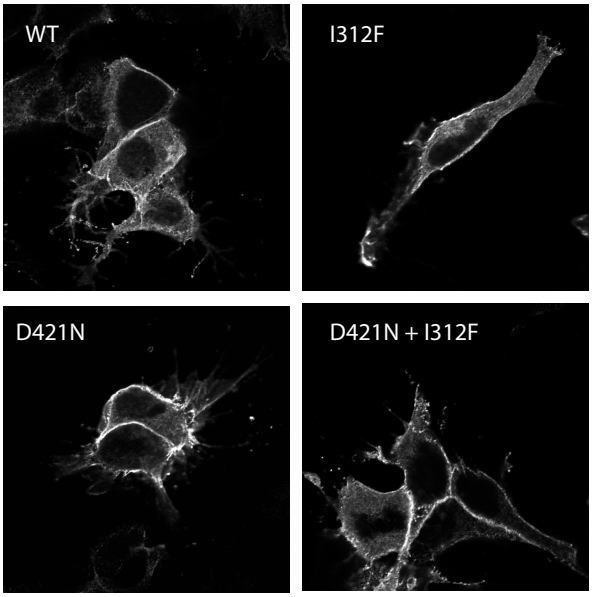

Supplementary Figure S4

Cellular distribution of WT DAT, DAT-I312F, and DAT-D421N in transiently transfected HEK293 cells. DAT was visualized by immunostaining with an N-terminal antibody. We observed clear labeling of the plasma membrane, for both WT and mutant transfected cells, as well as labeling of transporters in intracellular compartments. The images are representative of three independent experiments.

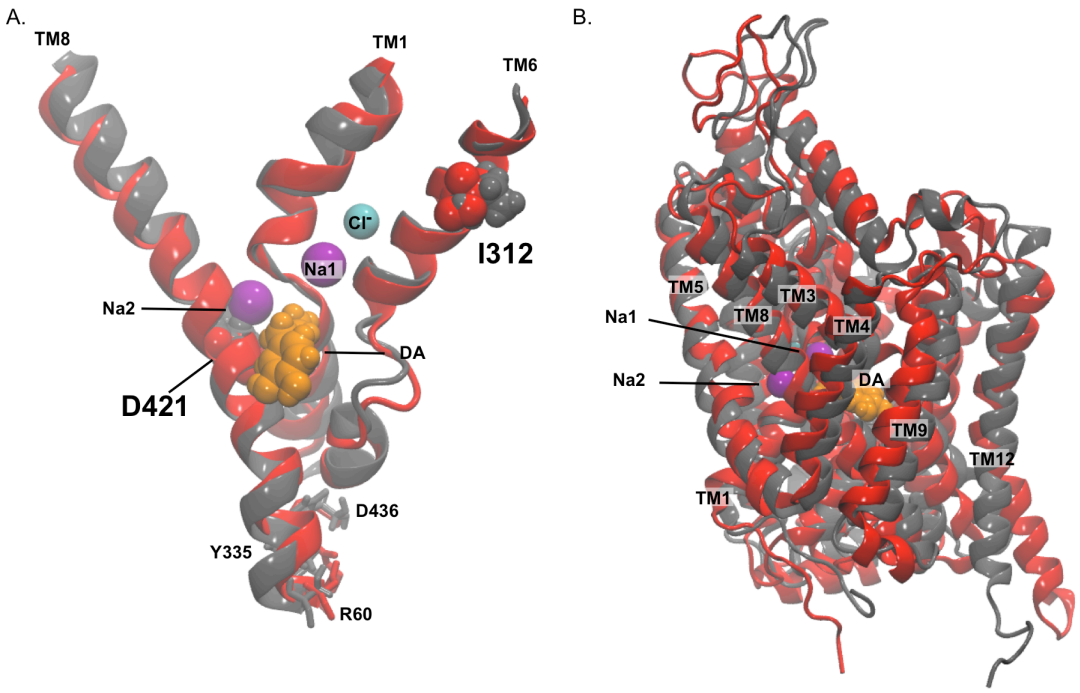

Supplementary Figure S5

Superimposition of the molecular models of hDAT. (A) Homology model of hDAT based on the outward-open crystal structure of LeuT (grey) superimposed on the homology model of hDAT based on the crystal structure of *Drosophila melanogaster* dopamine transporter (red). (B) Superimposition of critical residues within and surrounding the substrate and ion binding sites in both models. Sodium and chloride ions are indicated in purple and turquoise respectively. The Root Mean Square Deviation (RMSD) between hDAT based on LeuT (grey) and dDAT (red) is 1.3Å for the critical residues in TMs 1, 6 & 8 and 1.9Å for TM1-10.

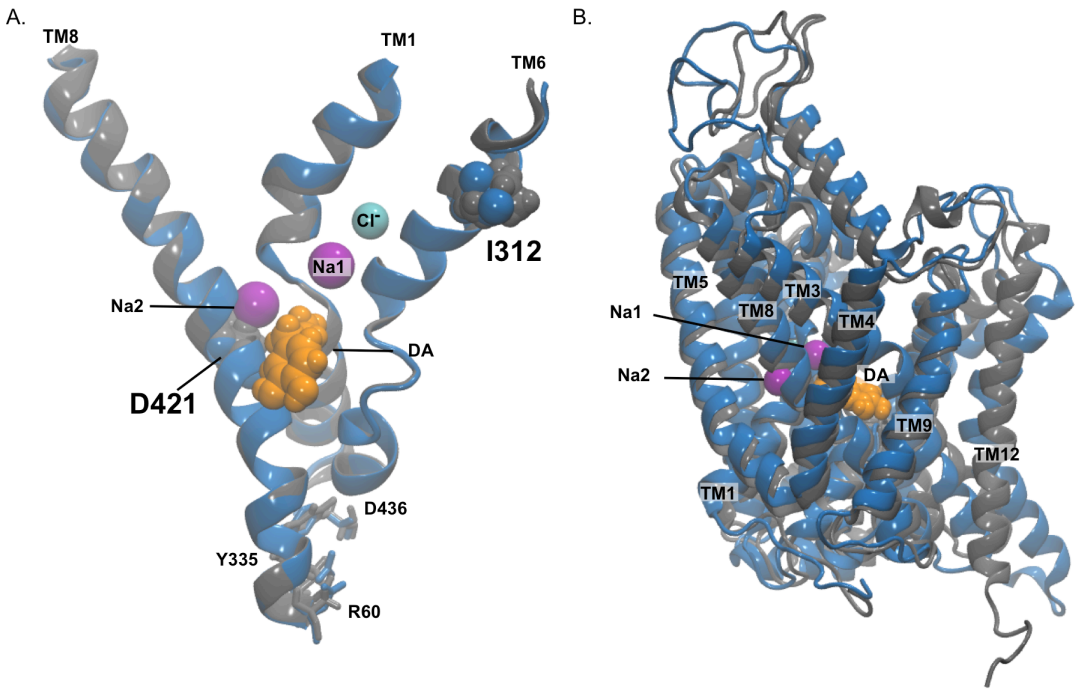

Supplementary Figure S6

Superimposition of molecular model of hDAT, based on the outward-open crystal structure of LeuT, PDB ID: 3TT1, and a homology hybrid model of hDAT, based on LeuT for TMs1-10 and dDAT for TMs11-12. Penmatsa *et. al.* (1) reported that the core of dDAT closely resembles LeuT, but the *periphery* has very different features, including a kink in TM12 (Supplementary Figure 3B), which makes the dimerization interface in dDAT very different from LeuT. (A) Superimposition of critical residues within and surrounding the substrate and ion binding sites in both models. Sodium and chloride ions are indicated in purple and turquoise respectively. (B) The hybrid model of hDAT (in blue) has a negligible Root Mean Square Deviation of 0.3Å from the hDAT model based on LeuT (grey) for critical residues in TMs 1, 6 & 8; for TMs1-10 it is 0.4Å. This further justifies the use of the LeuT based model for this particular study focusing on the substrate and ion binding sites.

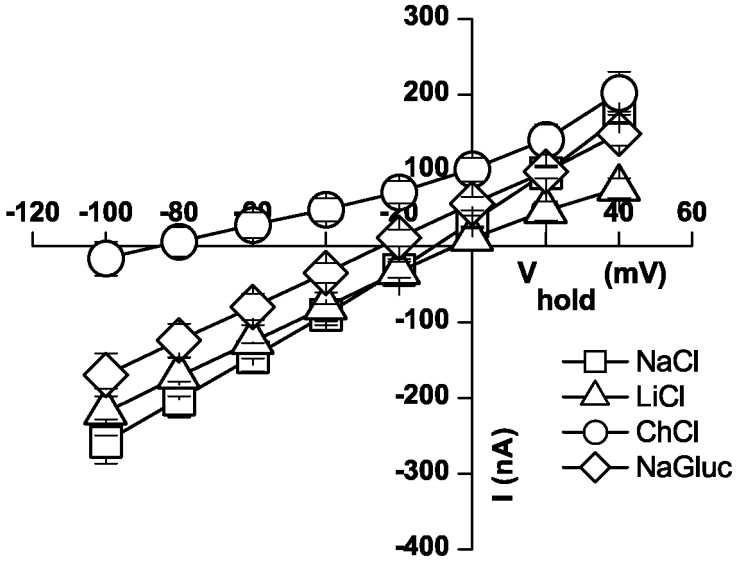

Supplementary Figure S7

Ion substitution experiments for DAT-D421N suggest that the cocaine-sensitive leak is primarily carried by cations. The I/V diagram shows the cocaine-sensitive (control-cocaine) steady-state leak current in NaCl (squares), LiCl (triangles), choline chloride (ChCl, circles) and sodium gluconate (NaGluc, diamonds). WT and mutant constructs were expressed in *Xenopus* oocytes and analyzed by the two-electrode voltage clamp technique as described in Materials and Methods. The I/V diagrams were generated in 20 mV steps from -100 to +40mV. Data are means ± s.e.m, n= 3-4). The DAT-D421N leak current is primarily carried by sodium, because the reversal potential changes dramatically by substituting sodium with choline. In contrast, the reversal potential hardly changes when choline is substituted to gluconate, indicating that the current was not carried by anions. .

Exon	Forward primer	Reverse primer
2	tggctgaagaccaagaggg	ctcgtttccgtacgtgcc
3	atggatggttgactggggta	ccatgcctgtgtcttagcaa
4	tgggctcagggtaatgtctc	ccagagcactaaagggatgg
5	agttccaggtgggttgacag	agcacaaaacccaactgagg
6	ctcccaatcagaggacaagc	ggcaatgcatatggaaacct
7	agggtgctcaggtcctttg	gctgtcgcttctgtctgaaa
8	aaaagtagcccctccgaaga	caaggaaaaaggctttgctg
9	caggatgggcgggagag	cccagggatcttgcctagc
10	gtcctcactaccaggcatcc	gatgtgcagttaccctgtgc
11	gtgtgcacagtgaatccc	gaaaggtgtttcctcacgg
12	ggacactgatgccacctctt	gactccagccacagtgacaa
13	cctgctttgtcctggcac	cacggagcctttctggtg
14	ggtgagggtgctggtaggt	gcacatgctggctgagtaaa
15	tcagctgctcttaaatgggg	gggagcctcacagagaca

Supplementary Table 1

Unique primer sequences used for sequencing the *SLC6A3* exons. Primers for exon 1 are not included as this exon is non-coding and therefore not analyzed. To make the sequencing procedure efficient, all forward primers had a tail of: acccactgcttactggcttatc and all reverse primers had a tail of: gaggggcaaacaacagatggc. The tails are not shown in the table.

1. Penmatsa, A., Wang, K.H., and Gouaux, E. X-ray structure of dopamine transporter elucidates antidepressant mechanism. *Nature*. 2013:1-7.